International Conference on Mathematics, Computational Methods & Reactor Physics (M&C 2009)
Saratoga Springs, New York, May 3-7, 2009, on CD-ROM, American Nuclear Society, LaGrange Park, IL (2009)

AN AUTOMATED CROSS SECTION PARAMETRIZATION METHOD FOR MTR APPLICATION

R. H. Prinsloo [*] **, P. M. Bokov, G. Stander, D. Botes**
Necsa
Building 1900, Pelindaba
Pretoria, South Africa, 0001
rian.prinsloo@necsa.co.za

W. Joubert
PBMR
Centurion, South Africa
Wessel.Joubert@pbmr.co.za

ABSTRACT

The advent of more advanced MTR (Material Test Reactor) fuel and reactor designs necessitate a corresponding improvement in the cross-section representation models applied to few group homogenized diffusion parameters. This problem may be decomposed into the construction of an appropriate cross-section representation model (the definition of relevant state parameters and associated basis functions), and the subsequent determination of approximation coefficients. In this work a sparse grid - based global polynomial cross-section parameterization method is presented which addresses both these aspects. A technique known as analysis of variance (ANOVA) is applied to construct the model and an efficient sparse grid integration scheme is implemented to determine the expansion coefficients. The method has a number of advantages, such as: built-in error control; consistent treatment and importance evaluation of all state parameters, including burn-up; and identification and approximation of all cross-section dependencies, including cross-terms. The method is applied to different MTR fuel designs and compared to more traditional MTR parameterization methods. The usefulness of the method as both model building- and few-group, cross-section reconstruction tool, is illustrated.

Key Words: Cross-section parameterization, diffusion parameters, sparse grid

1. INTRODUCTION

Material Test Reactor (MTR) designs are evolving as new design requirements include higher power, increased U-235 loading, the usage of low enriched uranium (LEU) fuel with burnable poisons and an increased number of in-core irradiation positions. All of these factors place more stringent requirements on the calculational tools which support reactor operation. One such aspect of the typical reactor calculational path is the definition of an appropriate cross-section representation model, and the calculation of the corresponding regression coefficients, as applied to few group homogenized diffusion parameters.

Few-group homogenized cross-sections are typically pre-calculated, parameterized and stored in representations such as tables or polynomial libraries. It would of course be preferable to

[*] Corresponding author

calculate these cross-sections online, allowing the transport solver to determine the node-averaged cross-section exactly for the state conditions of the given node within the core, but this approach generally proves to be computationally too expensive, especially during transient calculations. On the other hand, the construction of such multi-dimensional parameterized libraries requires an in-depth knowledge and understanding of the physics of the problem and involves extensive analysis of cross-section dependencies, which, for complex systems, may be a daunting and time-consuming task. Furthermore, the practicality of such a library is measured by its associated accuracy, cross-section reconstruction time and storage requirements.

Typically, MTR fuel cross-sections are parameterized against burn-up, fuel temperature, moderator density and moderator temperature. The mentioned advances in MTR reactor designs potentially complicate few-group cross-section dependencies and introduce a number of alternative or additional candidates as potential state parameters. These may include spectral indices and/or absorber number densities (xenon or burnable poisons). It is important to evaluate various cross-section representations in order to simplify representation models and hence, eventually, improve the reconstruction time of the diffusion parameters during global reactor calculations.

In this work previous developments [1,2] are extended and a method is proposed which addresses the need for more flexible, automated LWR/MTR cross-section parameterization, while maintaining control of the parameterization error. This approach employs a global, multi-dimensional approximation which can capture unknown and intricate few group cross-section dependencies in an automated fashion, and allows evaluation of various state parameters to determine the appropriate dimensionality of the cross-section model.

Recently such a method of cross-section parameterization was developed by Bokov and Prinsloo [1] based on a quasi-regression (QR) parameterization technique. This QR approach makes use of quasi-Monte Carlo integration to obtain regression coefficients and applies analysis of variance (ANOVA) as a technique for sensitivity analysis [2]. Although very general, this method of integration requires a large amount of transport calculations for estimation of the regression coefficients. In order to address this issue, and make the methodology more practical for day to day calculations of MTRs and LWRs, a sparse grid (SG) based integrator has now been implemented which requires substantially fewer (multiple orders) transport calculations to perform the multi-dimensional integration required to determine the regression coefficients. This development is described in the next section.

The same strengths regarding sensitivity analysis of appropriate expansion terms and state parameters remain within this SG based approach, as was demonstrated for QR in [2]. Furthermore, burn-up is no longer treated as base dependence which should be fitted separately, as is often the case, but may now be seen as simply another state parameter evaluated for its importance to cross-section reconstruction. In this paper, the ability of this methodology to build an appropriate representation model, and estimate the regression coefficients will be demonstrated on two different problems; the first being a typical MTR fuel element design, and the second a more advanced and neutronically difficult MTR design containing burnable poisons.

2. METHODOLOGY DESCRIPTION

Consider the dependencies of a few-group neutron cross-section F on d state parameters x_i within a multi-dimensional rectangular problem domain $D^d = \{\mathbf{x} \in \mathbb{R}^d : a_i \le x_i \le b_i, 1 \le i \le d\}$ which is mapped, for convenience, onto a unit hypercube $I^d = \{\mathbf{u} \in \mathbb{R}^d : \ 0 \le u_i \le 1, \ 1 \le i \le d\}$. The function $F(\mathbf{u})$ is approximated by a linear combination

$$F_\Omega(\mathbf{u}) = \sum_{\mathbf{k} \in \Omega} \beta_{\mathbf{k}} \psi_{\mathbf{k}}(\mathbf{u}) \tag{1}$$

of orthonormal multivariate basis functions $\psi_{\mathbf{k}}(\mathbf{u})$ built as a tensor product $\psi_{\mathbf{k}}(\mathbf{u}) = \prod_{i=1}^{d} \phi_{k_i}(u_i)$ of orthonormal univariate functions $\phi_{k_i}(u_i)$, which are constructed by normalization $\phi_k(u) = P_k^*(u) \,/\, \left\| P_k^*(u) \right\|_2$ of the shifted Legendre polynomials $P_k^*(u)$, where $\left\| P_k^*(u) \right\|_2 = \left[\int_0^1 \left(P_k^*(u) \right)^2 du \right]$. The index vectors $\mathbf{k} \in \mathbb{Z}_+^d$ contain d nonnegative integers representing the orders of the polynomials. Different combinations of indices k_i will lead to an infinite set $\Omega^{(\infty)}$ of index vectors from which a subset Ω of low-order terms is used in practice.

As it is demonstrated in [4] the regression coefficients minimizing the least-square error can then be calculated as follows:

$$\beta_{\mathbf{k}} = \int_{I^d} F(\mathbf{u}) \psi_{\mathbf{k}}(\mathbf{u}) d\mathbf{u}, \ \ \mathbf{k} \in \Omega. \tag{2}$$

The critical issue in the problem of approximation using model (1) is numerical integration of multivariate functions over the multi-dimensional problem domain as in (2). Multi-dimensional quadratures, built as a tensor product of one-dimensional quadrature rules, become impractical when the number of parameters exceeds 3 or 4 because of exponential growth of the computational cost with number of dimensions d (the so-called *curse of dimensionality*).

Therefore, for application to cross-section parameterization where the number of state parameters can often be in excess of 4, a method which does not suffer from this problem, should be applied. A Monte Carlo technique called quasi-regression, using Sobol' sequence of low discrepancy points (quasi-Monte Carlo integration), has been suggested previously in this regard [1,2]. These studies demonstrated its potential for cross-section parameterization, but quasi-Monte Carlo quadrature can still require an unacceptably large number of function calls. On the other hand, based on practical experience, it is known that the dependence of few-group neutron cross-sections on most state parameters can be described with low order polynomials. This leads

us toward an idea of replacing the integration rule with a Sparse Grid (SG) integration rule, while the bulk of the methodology remains as described in [2], namely that the optimization of the model is based on ANOVA which states that contribution of a particular term in the sum (1) to the function variance is equal to $\beta_{\mathbf{k}}^2$. This allows us to carry out different manipulation (such as rejection of terms in (1), rejection of state parameters etc.) with the model, while keeping control over the error induced by these manipulations. This feature is what is referred to as *error control* in the paper.

The SG integration allows extending the use of univariate quadrature rules to multiple dimensions with a substantially lower number of function evaluations compared to the tensor product rule. This is achieved by combining univariate quadrature rules of different accuracy levels in the tensor product, instead of having the univariate rules of the same accuracy as in the classical use of the tensor product [5]. Let us summarize SG integration used in this work. Assume a sequence of univariate quadrature formulas

$$Q^l\left[f\right] = \sum_{j=1}^{m_j} w_j^l \cdot f\left(u_j^l\right) \tag{3}$$

with $m_l \in \mathbb{N}$ is given. Let us use the following notations: $\Delta^l = Q^l - Q^{l-1}$ for the *accuracy level* $l \in \mathbb{N}$, where $Q^0 = 0$; $\left\|\mathbf{l}\right\|_1 = l_1 + \ldots + l_d$ for $\mathbf{l} \in \mathbb{N}^d$. The increase of the accuracy level is used for improving the approximation, with each subsequent level requiring additional sample points for evaluation. Assume $f_{\mathbf{k}}\left(\mathbf{u}\right) = F(\mathbf{u})\psi_{\mathbf{k}}(\mathbf{u})$. The approximation of the integral (2) using SG integration based on univariate rules Q^l is defined for a $q \geq d$ as a linear functional

$$\hat{\beta}_{\mathbf{k}}^{(q)} = \sum_{\left\|\mathbf{l}\right\|_1 \leq q} A(q,d)\left[F(\mathbf{u})\psi_{\mathbf{k}}(\mathbf{u})\right], \tag{4}$$

defined as follows: $A(q,d) = (\Delta^{l_1} \otimes \cdots \otimes \Delta^{l_d})$. In the paper we use the convention that "hat" symbol denotes an estimate of the corresponding variable.

The tensor product algorithm (4) is based on the multidimensional grid $U^{l_1} \times \cdots \times U^{l_d}$, where '$\times$' denotes the Cartesian product of the sets of univariate nodes defined as $U^l = \{u_1^l, \ldots, u_{m_l}^l\} \subset [0,1]$ that correspond to the applied quadrature rules Q^l. In this work it is assumed that the univariate nodes are nested $U^l \subset U^{l+1}$, and therefore the linear functional in (4) depends on function values at the union

$$H(q,d) = \bigcup_{\left\|\mathbf{l}\right\|_1 = q} \left(U^{l_1} \times \cdots \times U^{l_d}\right) \tag{5}$$

with $H(q,d) \subset H(q+1,d)$. We used the Clenshaw-Curtis quadrature rule in (3), where the nodes are u_j^l and the weight w_j^l $(j = 1,\ldots,m_l,\ m_l > 1)$ are chosen by the demand that Q^l is exact for all polynomials of degree less then m_l, where $m_0 = 1$ and $m_l = 2^{l-1} + 1$ for $l > 0$.

To illustrate the above formulae we give an example of a two-dimensional SG in Figure 1. This example is based on the Clenshaw-Curtis quadrature rule and includes sparse grid points up to accuracy level 4.

The following relationship

$$\int_{I^d} F^2(\mathbf{u}) d\mathbf{u} = \sum_{\mathbf{k} \in \Omega^\infty} \beta_{\mathbf{k}}^2 , \tag{6}$$

which is a multidimensional analogue of the famous Parseval's theorem, will be useful for error analysis. Let

$$\mathrm{E}\left[F(\mathbf{u})\right] = \int_{I^d} F(\mathbf{u}) d\mathbf{u}, \quad \mathrm{Var}\left[F(\mathbf{u})\right] = \mathrm{E}\left[\left(F(\mathbf{u}) - \mathrm{E}\left[F(\mathbf{u})\right]\right)^2\right] \quad \text{and} \quad \mathrm{ISE} = \int_{I^d} \left(F(\mathbf{u}) - F_\Omega(\mathbf{u})\right)^2 d\mathbf{u} \tag{7}$$

be the expectation (average), variance and Integrated Squared Error (ISE) of function $F(\mathbf{u})$, correspondingly.

Then, from formulae (1-2,6) follows

$$\mathrm{E}\left[F(\mathbf{u})\right] = \beta_{\mathbf{0}}, \quad \mathrm{Var}\left[F(\mathbf{u})\right] = \sum\nolimits_{\mathbf{k} \in (\Omega^{(\infty)} \setminus \mathbf{0})} \beta_{\mathbf{k}}^2 \quad \text{and} \quad \mathrm{ISE} = \sum\nolimits_{\mathbf{k} \notin \Omega} \beta_{\mathbf{k}}^2 . \tag{8}$$

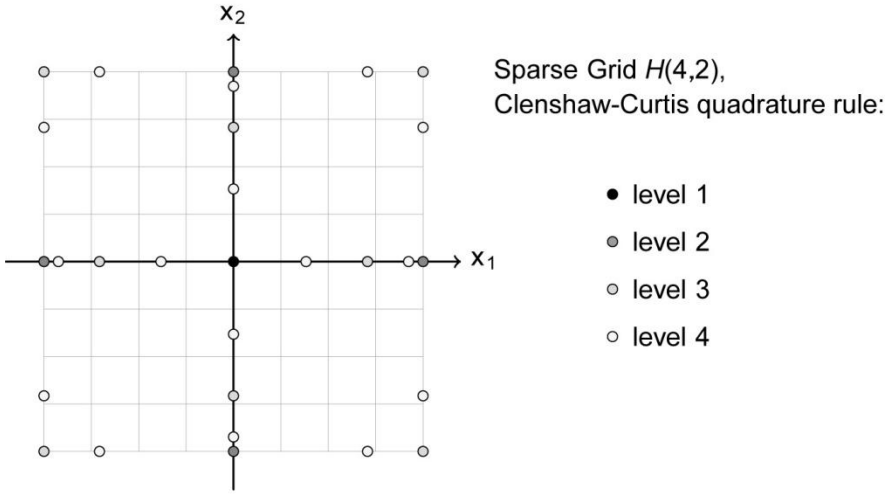

Figure 1. Example of Clenshaw-Curtis sparse grid in two-dimensional case

Note, that the formulae above state that the variance is a sum of squared expansion coefficients (except constant term), and ISE is the sum of the squared coefficients that are not included in approximation formula (1) and therefore it describes the truncation error. In other words, given that the exact values of the regression coefficients are known, the truncation error can be estimated via the difference between the variance and a sum of the squared coefficients included in the approximation. For practical situations, analogous to ISE, we define the Mean Squared Error (MSE) as

$$\mathrm{MSE} = \int_{I^d} \left(F(\mathbf{u}) - \sum\nolimits_{\mathbf{k}\in\Omega} \hat{\beta}_{\mathbf{k}}^{(q)} \psi_{\mathbf{k}}(\mathbf{u}) \right)^2 d\mathbf{u} \qquad . \tag{9}$$

which is obtained by substitution of estimators $\hat{\beta}_{\mathbf{k}}^{(q)}$ instead of the exact values $\beta_{\mathbf{k}}$ in (1) and (7). We now define our main error measure as Lack Of Fit (LOF), which may be interpreted as the unexplained part of the function variance. Hence

$$\mathrm{LOF} = \mathrm{MSE}/\mathrm{Var}\left[F(\mathbf{u})\right] \tag{10}$$

which we estimate via Lack of Variance (LOV):

$$\mathrm{LOV}^{(q)} = \frac{\hat{V}^{(q)} - \hat{X}^{(q)}}{\hat{V}^{(q)}} \tag{11}$$

with $\hat{X}^{(q)} = \sum_{\mathbf{k}\in\Omega^{(q)}} \left(\hat{\beta}_{\mathbf{k}}^{(q)}\right)^2$ being the explained part of the variance and $\hat{V}^{(q)}$ being the estimator for the variance which is calculated via $\hat{V}^{(q)} \equiv \widehat{\mathrm{Var}}\left[F(\mathbf{u})\right] = A(q,d)\left[\left(F(\mathbf{u}) - \hat{\beta}_{\mathbf{0}}^{(q)}\right)^2\right]$.

The concept of improved accuracy with increasing level can be used as a practical error estimation of integration accuracy. Thus for an integral of an arbitrary function $g(\mathbf{u})$ defined over I^d the accuracy of the integration result (absolute error) can be calculated via $\left|\left(A(q,d) - A(q-1,d)\right)\left[g(\mathbf{u})\right]\right|$ and therefore $\hat{\varepsilon}^{(q)}\left(\hat{V}^{(q)}\right) = \left|\hat{V}^{(q)} - \hat{V}^{(q-1)}\right|$ and $\hat{\varepsilon}^{(q)}\left(\hat{\beta}_{\mathbf{k}}^{(q)}\right) = \left|\hat{\beta}_{\mathbf{k}}^{(q)} - \hat{\beta}_{\mathbf{k}}^{(q-1)}\right|$. Hence we calculate the error as an absolute value of the integral estimation as compared to the previous level.

In this paper, we have utilized the orthogonality of basis functions to determine the subset of terms calculated exactly for the current level, hence $\Omega^{(q)} = \left\{\mathbf{k} : A(q,d)\left[\psi_{\mathbf{k}}^2(\mathbf{u})\right] = 1\right\}$. This is selected so that all terms kept within the level *q* approximation are exact.

3. PROBLEM AND CODE DESCRIPTION

The described methodology will be applied to two fuel designs, the first (Fuel A) representing a typical MTR plate type fuel assembly containing high enriched uranium (HEU), and the second a more advanced LEU MTR fuel design containing burnable poisons in the side plates (Fuel B). The aim of the analysis would be to investigate appropriate cross-section models and calculate regression coefficients for both fuel types. Transport solutions at required state points will be carried out via the collision probability based HEADE code, which forms part of the OSCAR [3] calculational system. The SG based parameterization methodology has been implemented into a test code named SPARX. The SPARX code performs the following functions:

1. Generate a *n*-dimensional, level *l* sparse grid mesh on which transport calculations should be performed, after which the HEADE code is called to calculate macroscopic and microscopic homogenized multi-group cross-sections at the required state conditions on the SG mesh. Note that burn-up is included in this approach.
2. Perform the SG integration based on the obtained function values and calculate coefficients for all considered basis functions, including cross-terms, up to a prescribed order *m* of the approximation. In practice a limit is placed on the maximum uni-variate order, maximum total tensor-product order and number of interacting state parameters.
3. Calculate the contribution of each basis term to the variance of a given cross-section (given simply by the square of the coefficient , $\beta_{\mathbf{k}}^2$), and utilize this measure in deciding which basis functions should remain in the final cross-section representation. A built-in error measure is generated, defined by Lack of Variance (LOV), which essentially expresses the mean square error (MSE), calculated directly from the coefficients, as a fraction of function variance.
4. Evaluate the accuracy of the model by performing a post-regression evaluation of the predicted error, as well as estimating the average relative and maximum relative error, from an independent set of control points. This component is not part of the SG methodology, but is included in the SPARX code for verification of the produced library.

The SPARX code thus combines the building of a cross-section representation model (number of parameters, set of basis functions) with the generation of the regression coefficients. In this regard the SPARX code will provide information to assist in decisions such as which set of state parameters are appropriate, which order of polynomial approximation should be considered, how much cross-term dependence is present, and in which cases should a given dimension within the domain be considered for subdivision. In the SPARX code these decisions are based on the result of the ANOVA technique, which provides information regarding the importance of individual parameters and basis functions to the overall function dependence.

Results from the different models will also be compared to the existing four-dimensional (burn-up, moderator density, fuel and moderator temperature) representation model as applied in the POLX code within the OSCAR [3] system. The methodology implemented in the POLX code treats burn-up and the off-base state parameters (fuel temperature, moderator density and temperature) separately. The cross-section dependence on the off-base state parameters are fitted separately for each burn-up point using a single least squares quadratic polynomial fit per off-base parameter. The polynomial coefficients of each of these fits are then themselves fitted over

the burn-up range. The burn-up range may be subdivided iteratively, if required, to satisfy the error criteria. The main disadvantages of this methodology are the lack of direct error control for the initial off-base state parameter approximation and the inability to capture cross-terms between state parameters.

4. RESULTS AND DISCUSSION

As indicated, two fuel types will be calculated in this work, with the aim to investigate, via the SG methodology, appropriate cross-section models and determine reconstruction coefficients. In this regard both the creation time of such a library (dominated by the number of transport calculations), as well as the cross-section reconstruction time (dominated by the number of terms to assemble), is critical. The two fuel types under consideration are briefly summarized in Table I, with all state parameter ranges included.

Table I. Properties of fuel types A and B

Property	Type A	Type B
Fuel type	HEU Plate type	LEU Plate type
Enrichment	90%	19%
U-235 content	300 grams	570 grams
Broad groups	6	7
Burnable poison	None	42 Cd Wires
Burnup range	0 – 301 days	0 – 301 days
Fuel temp. range	293 K – 453 K	318 K – 478 K
Moderator temp. range	298 K – 398 K	303 K – 403 K
Moderator dens. Range	0.693 – 1.002	0.687 – 0.997
Xe Number Dens. Range	0 – 3E-08	0 – 3E-08

4.1. Fuel Type A

A typical set of MTR state parameters will be applied to produce an initial 4-dimensional SPARX model for “Fuel Type A” in order to illustrate the basic functionality of the methodology. The state parameters utilized in the 4D model are burn-up, fuel temperature, moderator temperature and moderator density. As illustration, an extract of the typical information produced by the SPARX code is shown in Table II for the U-235 group 6 absorption microscopic cross-section for a level 6 calculation. The concept of the sparse grid level (see definition of l in (3)) essentially indicates how many times the range is subdivided in terms of the number of sample points required. At this point a relatively low sparse grid level is chosen (compared to the dimensionality of the problem) for an initial investigation of the unknown cross-section dependencies.

Table II. Extract from 4-D U-235 group 6 SPARX absorption model

Basis Function	Coefficient	Contribution, %
(0 0 0 0)	7.06E+01	
(1 0 0 0)	2.98E+00	70.88%
(0 0 1 0)	-1.82E+00	26.50%
(0 0 0 1)	3.74E-01	1.11%
(2 0 0 0)	2.76E-01	0.61%
(1 0 1 0)	-3.05E-01	0.74%
(0 0 2 0)	9.73E-02	0.08%

In Table II entries in the "Basis Function" column contain four indices which denote the order of the polynomial basis functions in the four state parameter dimensions. Hence the 6^{th} term (1,0,1,0) denotes a bi-linear cross-term between burn-up and moderator temperature and contributes 0.74% to the variance of the global approximation function. The coefficients used for reconstruction of the cross-sections, according to (1), are given in column 2. Table II shows only an extract of the full level 6 representation, which was limited to a maximum polynomial order of nine and contained 22 terms in total. Table I provides valuable information regarding the importance of the various basis functions and state parameters, and potentially, which state parameters are unimportant and hence may be neglected [2]. The importance of a given state parameter may be gauged from the sum of importances of the basis terms with a non-zero entry in the given parameters index. As an example, based on the on the data presented in Table I, the importance of the moderator dimension to the overall function dependence is 27.32% (26.5% + 0.74% + 0.08%).

An initial investigation into the accuracy of this level 6 model is shown in Table III for the microscopic 6-group U-235 absorption cross-sections.

Table III. Multi-group errors of 4D SPARX parameterization model (%)

	Library	Independent test		
Cross-section	**Predicted LOV %**	**LOF,%**	**Average relative error, %**	**Maximum relative error, %**
U-235 abs gr. 1	7.99E-04	5.14E-04	1.55E-03	8.55E-03
U-235 abs gr. 2	7.38E-04	1.70E-03	5.28E-04	3.21E-03
U-235 abs gr. 3	6.16E-05	5.55E-05	1.21E-03	7.55E-03
U-235 abs gr. 4	3.30E-04	3.39E-04	2.55E-04	3.38E-03
U-235 abs gr. 5	1.30E-02	1.79E-02	2.54E-02	3.17E-01
U-235 abs gr. 6	1.10E-02	6.47E-03	2.53E-02	6.81E-01

The question of whether the produced representation model is sufficiently accurate may now be investigated. Table III shows a range of errors measures for the U-235 multi-group absorption cross-sections. The Lack Of Variance (LOV) error measure in column two indicates the percentage of the function variance not described by the model (truncation error in (1)), which is calculated during the library creation process directly from the coefficients [1,2]. The error measures in columns three to five are generated during the independent post-regression evaluation of the library and rely on a statistical sample of points (generated in this case from a low-discrepancy (quasi random Sobol) sequence – 16384 points in this case). The reference spans 4-dimensional space and tracks the depletion of a fresh fuel element over its lifetime. Column three shows the post-regression Lack Of Fit (LOF) estimator, which aims to reproduce, statistically, the analytical library based LOV error measure.

For ease of analysis, we will focus further discussion on the group 6 cross-section (largest error), and defer comments on the errors listed in Table III to Table IV. Of course the approach followed here should be applied to all relevant cross-sections needed for the global diffusion problem in a practical application.

Table IV. U-235 group 6 errors of 4D SPARX parameterization model

	Library		**Independent test**			
Sparse Grid level *Max Order 9*	**Predicted LOV, %**	**Number of Terms**	**LOF, %**	**Average relative error, %**	**Maximum relative. Error, %**	**Nr. of Transport calls**
5	2.98E-2	13	2.72E-2	6.84E-2	6.16E-1	401
6	1.10E-2	22	6.47E-3	2.53E-2	6.81E-1	1105
7	3.05E-3	25	2.98E-3	1.78E-2	6.90E-1	2929
8	1.53E-3	31	1.41E-3	8.52E-3	6.46E-1	7537
POLX (4D)	--	147	--	2.21E-2	1.02E-1	301

Table IV addresses the first typical approach within the SG methodology of improving reconstruction errors. The calculation for the group 6 absorption cross-section is repeated for various sparse grid levels. Each level requires a different number of transport calculations to generate coefficients. Table IV illustrates how the approximation error diminishes with increased order of the sparse grid, which translates into an increasing number of expansion coefficients, with increasing orders, calculated exactly. As stated, the level 6 sparse grid library contains only 22 terms for this cross-section, whereas the level 8 calculation contains 31. Further it is important to note that the library predicted LOV agrees relatively well with the post regression estimate, and hence may be used as a guideline for the accuracy of the produced library in a mean-squared sense. On the other hand, the maximum relative errors for all levels are high as compared the typical parameterization error target of around 0.1%, and further investigation is needed to construct a practical library.

The final entry in the table lists the POLX result. It should be noted that the large number of terms (147) are needed to represent the subdivided burn-up range. The number of terms used in the actual reconstruction of the cross-section, assuming that the correct burn-up segment has been found, is only 21 (7 burn-up subdivision). In the case of the SG approach all terms used in the representation is needed for reconstruction. The POLX accuracy is good due to the domain splitting and requires a small number of transport calculations. On the other hand, no off-base interaction terms will be captured by POLX, and any significant contribution in this regard will place an upper limit on the accuracy of the approach.

The SG methodology constructs a global fit over the full 4D approximation space, with the assumption that the cross-section dependence is reasonably smooth. Strong local function behavior within state space is the typical reason for excessive maximum errors, as can be seen in Table IV with maximum cross-section errors reaching 0.7% for all orders. The SPARX method supports the identification of such local behavior by identifying the parameter which require the highest order fit, and then using the existing sparse grid points to identify the approximate position of the maximum error within that parameter range.

In this case the burn-up dimension was noted to require all expansion terms up to order nine, and the region of maximum error was identified to be within the first half of the burn-up range. Within the SPARX methodology, three possibilities now exist, the first two of which may be automated:

1. Increase the order of the approximation in the hope of capturing the local behavior
2. Subdivide the domain and generate multiple libraries. This approach makes the local behavior global within the subdivided domain, and the information regarding potential split points from the full domain calculation may be used to subdivide the domain.
3. If analysis of the result, combined with information regarding the region of maximum error, identifies the source of the local behavior, additional state parameters may be introduced to smooth the local behavior.

If the decision was taken to split the first half of the domain according to the SPARX suggestion and subsequently produce two level 6 libraries, the maximum errors improve to 0.31% as compared to the 4D level 8 value of 0.65%. The implication hereof is that an additional decision making level is needed in the global diffusion solver to select the appropriate library to reconstruct.

On the other hand, since the errors are found to be within the first half of the burn-up dimension, they are possibly as a result of the strong local Xe-135 behaviour at beginning of life of the assembly. To investigate this possibility we may choose to add Xe-135 number density (ND) as a state parameter. Table V summarizes the errors for a 5-dimensional approximation for fuel type A. The addition of Xenon ND as a state parameter also improves the functionality of the final library; varying Xenon concentration for all burn-up allows more accurate modeling of reactor scrams and restarts. Results in Table V show significant improvement, with the maximum error decreasing, for the level 8 calculation, by about a factor of 7.

Table V. U-235 group 6 errors of 5D SPARX parameterization model (%)

	Library		Independent test			
Sparse Grid level *Max Order 9*	**Predicted LOV, %**	**Number of Terms**	**LOF, %**	**Average relative error, %**	**Maximum relative. Error, %**	**Nr. of Transport calls**
5	9.20E-3	25	3.16E-2	6.03E-2	5.69E-1	801
6	2.40E-3	41	3.59E-3	1.84E-2	2.58E-1	2433
7	2.60E-3	51	5.83E-3	2.45E-2	5.18E-1	6993
8	2.65E-4	55	3.97E-4	5.93E-3	1.26E-1	19313

Also note that with the addition of an extra state parameter, the number of transport evaluations required merely doubled (compare Table IV). This is a property of the SG integrator and supports the conclusions that large numbers of state parameters may be utilized without experiencing the so-called "curse of dimensionality". An investigation into the library structure of the 5D approach shows that the high orders in the burn-up dimension have been replaced be a couple of low order terms in the Xenon dimension, with the linear term contributing a substantial 17% of the full function variance. We may conclude that the addition of the Xe ND as an additional state parameter is a good choice for "Fuel Type A".

As final comment regarding Table V, note that the same reference set of control points as in Table IV is used for the post-regression analysis. The Xenon number density was thus not varied independently, but given as its deterministic value at the given point during the depletion. This choice was made to allow comparison of the maximum and relative error in both tables and it is important to highlight that the predicted 5D LOV estimation is therefore no longer directly comparable to the post-regression LOF.

4.2. Fuel Type B

Fuel type B represents a more difficult problem, with Cadmium burnable poison wires inserted into the side-plates of the fuel design. Results for a 5D (already including Xenon as a state parameter) level scoping study for the U-235 absorption group 7 cross-section are shown in Table VI. The errors in this fuel design are substantially larger than those found without burnable poisons, and as an immediate potential remedy the maximum order of approximation terms were allowed to grow from 9 to 15 and then 25. The results from these cases are also included in Table VI.

In this case the increase in the approximation order proved successful in decreasing the error to acceptable levels. This indicates that the multi-dimensional dependencies were relatively complicated, but without sharp localized behavior. The POLX result is once again included, with

the large number of terms due to the large number of subdivisions performed on the burn-up range to meet the POLX fitting tolerance of 0.1%.

Table VI. Fuel B : U-235 group 6 errors of 5D SPARX parameterization model

	Library		Independent test		
Sparse Grid level	**Predicted LOV, %**	**Number of Terms**	**LOF, %**	**Average relative error, %**	**Maximum relative. Error, %**
5 (max order 9)	1.25E+1	14	1.55E+1	8.35E-1	2.55
6 (max order 9)	1.96E+1	31	3.15E+1	9.80E-1	8.49
7 (max order 9)	5.93E-1	40	7.64E-1	1.64E-1	7.84E-1
8 (max order 9)	5.85E-1	52	7.11E-1	1.56E-1	7.17E-1
8 (max order 15)	8.79E-2	65	1.21E-1	6.40E-2	3.29E-1
8 (max order 25)	7.57E-3	74	2.16E-2	2.74E-2	1.72E-1
POLX (4D)	--	882	--	1.37E-1	2.83E-1

To illustrate the nature of this dependence, Figure 2 shows the U-235 Group 7 absorption cross-section plotted against burn-up, for nominal conditions of all four the other state parameters. Included in the plot is the reconstructed cross-section for two cases: maximum order limited to 9, and limited to 25.

Figure 2 clearly shows the complicated variation in the microscopic U-235 cross-section, which is largely due to the spectrum effect of the burnable poison. From the figure the significant improvement in both relative and maximum error with increased order is also clearly visible.

It is clear that a 25 order cross-section library is not a practical solution, but improvement in the error does suggest that the method is capable of approximating intricate cross-section dependencies with its global approach. Nevertheless, this should be seen as an indication that some phenomena are not adequately covered by the selected state parameters, and not that the physics of the problem requires 25^{th} order expansions.

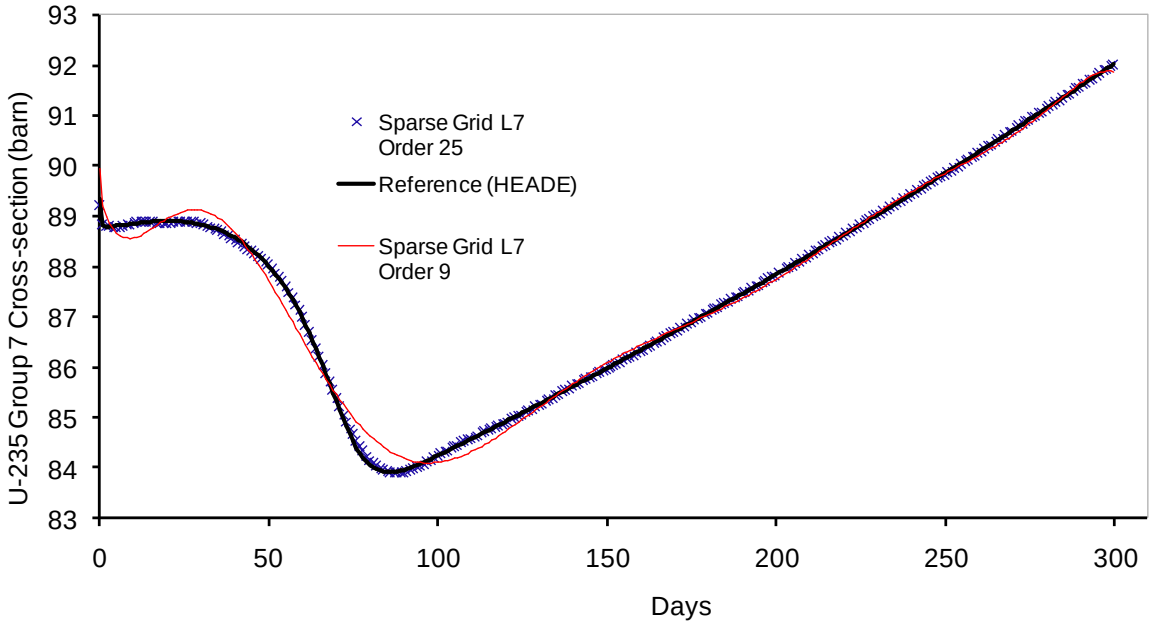

Figure 2. U-235 group 7 absorption cross-section vs. burn-up

For interest, the penalty in reconstruction time due to such a high order representation is estimated in Table VII, which compares the reconstruction times for various orders, based on the time required to fit a set of 1000 control points.

Table VII. Comparison in reconstruction time: 5D Fuel B model

Case	Number of Terms	Relative reconstruction time
Level 6 Max order 9	31	9
Level 8 Max order 9	52	16
Level 8 Max order 15	65	20
Level 8 Max order 25	74	25

From Table VII one may deduce that the reconstruction time scales near linearly with the number of terms in the approximation. For "Fuel type B" it may thus be advisable to split the domain into a few regions and subsequently diminish the order of the approximation, or potentially investigate additional spectral state parameters to capture the effect of the burnable poison. These studies are left for future work, but have been identified by a simple application of

the methodology. Furthermore, coupling and extensive practical testing of the method within the OSCAR-4 global diffusion environment will be the next natural step in the development.

5. CONCLUSIONS

The sparse grid based, cross-section parameterization methodology is presented in this work, and applied to cases of typical MTR plate type HEU fuel and LEU fuel, the latter containing burnable poisons. These examples provide some insight into how the sparse grid methodology can be used as both a model building and cross-section representation tool. The methodology provides flexibility in structure, order and computational cost while invaluable information is naturally supplied regarding the nature and complexity of the cross-section dependencies under consideration. The method allows for large numbers of state parameters, and does not suffer the typical curse of dimensionality regarding the number of transport calculations required.

Essentially, the sparse grid parameterization method combined with the ANOVA technique for sensitivity analysis allows an almost black box approach to the construction of a representation model for a given set of supplied state parameters, and the calculation of regression coefficients. The method has the ability to indicate which state parameters may be neglected, which are critically important, and which contain strong local behavior which should be addressed.

Furthermore, the approach provides a built in analytic error measure which has been proven to provide an excellent indication of the mean squared error of the fit. The next natural phase in the development would be to couple the methodology to the global diffusion solver in the OSCAR-4 code system and evaluate the efficiency and accuracy of the approach for practical application.

REFERENCES

1. P. M. Bokov, R. Prinsloo, “Cross-Section Parameterization Using Quasi-Regression Approach,”. *Joint International Topical Meeting on Mathematics & Computation and Supercomputing in Nuclear Applications (M&C + SNA 2007),* Monterey, California, April 15-19 (2007).
2. P. M. Bokov, et al., “A quasi-regression method for automated cross-section parameterization: PBMR benchmark example,” *Proceedings of PHYSOR 2008,* Interlaken, Switzerland, September (2008).
3. E.Z. Muller, et al., “Development of a Core Follow Calculation System for Research Reactors,” *Proceedings of the 9th Pacific Basin Nuclear Conference*, Sydney, Australia, 1-6 May (1994).
4. J. An, A. B. Owen, “Quasi-Regression,” *Journal of complexity* **17**(4), pp. 588-607 (2001).
5. E. Novak, K. Ritter, “High dimensional integration of smooth functions over cubes,” *Numer. Math*. **75**, pp. 79-97 (1996).